




INSTRUCTIONAL LABORATORIES AND DEMONSTRATIONS | MAY 01 2025

From light emission to solar power: Experiment on LED's photovoltaic behavior

Tiago V. Fernandes  ; Luís P. Gonçalves  ; Rodrigo Rito 



Am. J. Phys. 93, 422–429 (2025)

<https://doi.org/10.1119/5.0252410>



Learn about the newest
AAPT member benefit



INSTRUCTIONAL LABORATORIES AND DEMONSTRATIONS

John Essick, *Editor*

Department of Physics, Reed College, Portland, OR 97202

Articles in this section deal with new ideas and techniques for instructional laboratory experiments, for demonstrations, and for equipment that can be used in either. Although these facets of instruction also appear in regular articles, this section is for papers that primarily focus on equipment, materials, and how they are used in instruction. Manuscripts should be submitted using the web-based system that can be accessed via the American Journal of Physics home page, ajp.aapt.org, and will be forwarded to the IL&D editor for consideration.

From light emission to solar power: Experiment on LED's photovoltaic behavior

Tiago V. Fernandes,^{a)}

Departamento de Física, Universidade de Aveiro, Campus Universitário de Santiago, 3810-193 Aveiro, Portugal and Inorganic Chemistry, Department of Chemistry—Ångström Laboratory, Uppsala University, Box 538, SE-751 21 Uppsala, Sweden

Luís P. Gonçalves,^{b)} and Rodrigo Rito^{c)}

Departamento de Física, Universidade de Aveiro, Campus Universitário de Santiago, 3810-193 Aveiro, Portugal

(Received 9 December 2024; accepted 21 March 2025)

An experimental study to investigate the fundamental similarities between light-emitting diodes (LEDs) and solar cells (SCs) for educational purposes is here presented. Through a hands-on experiment using inexpensive, commercially available LEDs and simple laboratory equipment, students are introduced to characterization techniques, such as electroluminescence (EL) and current–voltage (I–V) measurements, as well as to optoelectronic devices, photovoltaic physics, spectroscopy, light-to-matter interactions, and solid-state physics concepts. Four LEDs of different colors—red, amber, green, and blue—are used in this study. The measured EL spectra allowed an estimation of the bandgap energy of the material constituting each LED's optical active layer, establishing a relationship with the LED color. Photovoltaic mode I–V curves are measured under outdoor sunlight, demonstrating that all LEDs exhibited photovoltaic behavior, generating electrical energy from incident light. The red LED produces sufficient electrical energy to power a small calculator, while the green LED exhibited the poorest photovoltaic performance. Shockley–Queisser (SQ) theory is employed to comparatively investigate the “photovoltaic” quantum efficiency (QE) of the LEDs, enabling students to relate the results to the well-known green gap problem in LED “emission” QE. This work effectively illustrates the similarities between LEDs and SCs, bridging the gap between theoretical knowledge and practical application, providing students with a valuable learning experience in solid-state physics, semiconductor-related topics, and photovoltaic technology. © 2025 Author(s). All article content, except where otherwise noted, is licensed under a Creative Commons Attribution-NonCommercial 4.0 International (CC BY-NC) license (<https://creativecommons.org/licenses/by-nc/4.0/>).

<https://doi.org/10.1119/5.0252410>

I. BACKGROUND

According to the United Nations Sustainable Development Goals, the energy sector urgently needs to transition from fossil-based energy sources to renewable, carbon-free alternatives. Renewable energy sources aim to produce energy through naturally sustainable means, such as solar energy, hydroelectricity, and wind energy. Among these, solar energy has seen the most significant development in recent years. The International Renewable Energy Agency (IRENA) reports substantial growth in the solar energy production capacity

worldwide, underscoring its critical role in the global energy landscape.¹ This transition marks a pivotal shift toward a more sustainable and environmentally friendly energy infrastructure.

Given this backdrop, it is imperative for university students, especially those in physics, engineering, and chemistry disciplines, to gain a deep understanding of how solar cells (SCs) work. In the literature, the importance of teaching photovoltaic physics to university students using different approaches and experiments has been highlighted.^{2–6} By comprehending the principles and technologies behind SCs, students can contribute to innovations and improvements in



this crucial field. Light-emitting diodes (LEDs) share similar principles with SCs in terms of their semiconductor properties and light-to-matter interactions. The experiment presented in this work enhances learning and prepares students to innovate in the photovoltaic energy sector.

LED devices have been extensively used for teaching physics, engineering, and chemistry-related topics, such as spectroscopy and electronic transitions, as well as the relationship between color, wavelength, and energy, in engaging ways for students.⁷ Additionally, fundamental concepts such as light absorption and emission in semiconductors, band theory, electron–hole pair generation, and light-emitting pn junctions have been explored in the context of LED and laser diode devices.⁸ Related to the present work, LEDs have been used as photodetectors in simple, low-cost “home-built” photometers,^{9,10} to demonstrate the relationship between wavelength and semiconductor energy level differences¹¹ and to investigate the intrinsic and extrinsic bandgaps, dopant materials, and diode design in LEDs.¹² Additionally, the potential of LEDs to generate electrical current under sunlight exposure has been exploited in water electrolysis processes.¹³ The idea that any pn junction can act either as a rectifier, LED, or SC had already been proposed and discussed for educational intent in another article.⁴ More recently, Barcellos and Oliveira demonstrated experimentally that common and commercially available red LEDs are capable of acting as SCs, providing energy generation to a small electrical device.¹⁴

Our study builds on and expands these previous concepts, providing new contributions to the field. Particularly, here, we investigate the photovoltaic behavior of LEDs of different colors through I–V measurements and relate the results to the bandgap energy of each LED’s active layer. While earlier works have demonstrated the photodetection and the potential photovoltaic behavior of LEDs, this study uniquely relates theoretical principles with the experimentally measured photovoltaic behavior, providing new insights into the LED’s photovoltaic efficiency in relation to Shockley–Queisser (SQ) theory and the green gap problem in LED technology. Using simple, inexpensive, and widely available LEDs, these advancements offer a convenient and comprehensive reference about the LEDs’ optoelectronic properties and a new approach to teaching photovoltaic physics and light-to-matter interactions in an engaging way.

II. INTRODUCTION

LEDs and SCs exhibit a significant degree of similarity. Aside from the use of a double heterojunction structure in modern LEDs, the fundamental structure of LEDs and SCs is the same. Both are optoelectronic devices based on semiconductor pn junctions, which are capable of converting electrical energy into optical energy and vice versa.^{15,16} Essentially, the differences originate from the distinct optimization undergone by LEDs and SCs to achieve their specific purposes. Thus, one can think of using a LED as a SC to produce electrical energy. By taking a laboratory experiment approach, this work aims to clarify concepts and extend the knowledge of undergraduate and graduate students about optoelectronic devices, photovoltaic behavior, spectroscopy, and, succinctly, solid-state physics.

To generate electrical energy, a SC’s absorber layer needs to absorb incident photons and create mobile charge carriers (electron–hole pairs), which are then separated and collected

at the electrical terminals of the device without significant loss of energy.¹⁵ Fundamentally, any pn junction can achieve this process, although with varying efficiency. In heterojunction SCs, the absorber layer is typically the semiconductor with the lowest bandgap energy (E_g). If a wider-bandgap semiconductor is positioned in front of the absorber layer, acting as either the p- or n- type region, it can absorb higher-energy photons, thereby reducing the number of photons reaching the absorber. Consequently, only the photons that successfully reach the absorber layer with energy equal to or greater than its bandgap will generate mobile charge carriers. It was based on this simple assumption, as well as on the solar spectral profile, that William Shockley and Hans Queisser developed a theory for solar cell optimization in 1961.¹⁷ This theory models the electrical behavior of a SC with a single absorber layer under standard AM1.5 illumination conditions. These conditions represent sunlight passing through (approximately) 1.5 times the Earth’s atmosphere thickness before reaching the surface and are characterized by an optical power density of 1000.4 W/m^2 and a specific spectral distribution that is shown in Fig. 1(a). As light travels a longer optical path through the atmosphere, scattering and absorption effects become more pronounced. This consideration arises because, for most practical applications, SCs do not operate under exactly one atmosphere’s thickness. Many of the world’s major population centers are located in temperate latitudes. Figure 1(a) also shows the blackbody spectrum at 5800 K, normalized to a power density of 1000.4 W/m^2 .

The SQ theory determines the theoretical maximum power density that a single-junction solar cell can achieve under standard AM1.5 illumination conditions, derived from the detailed balance between photon absorption and recombination. The model is based on four physical principles: (i) the absorption of photons will always occur if the photon energy is equal or greater than the bandgap energy of the SC’s absorber material; (ii) every absorbed photon will generate one electron–hole pair (free charge carriers), contributing to the photocurrent; (iii) all photogenerated charge carriers will thermalize to the band edges, and (iv) the only loss mechanism, despite the non-absorbed photons in (i) or the thermalization losses in (iii), is the spontaneous emission of photons by radiative recombination of free charge carriers.¹⁷ In agreement, the model predicts that the lower the bandgap energy of the absorber layer, the higher the generated short-circuit current density $J_{sc,SQ}$, as more photons are absorbed, while the open-circuit voltage $V_{oc,SQ}$ decreases due to lower collected energy per photon, as depicted in Fig. 1(b). Since the power output depends on both parameters, a detailed balance is considered. Consequently, the electrical power density $P_{max,SQ}$ that can theoretically be achieved by a single absorber layer SC is directly dependent on the bandgap energy of the semiconductor material that makes up the absorber layer and is maximized within the range of bandgap energies $E_g = 1.1\text{--}1.4 \text{ eV}$, as shown in Fig. 1(c). This result provides clear evidence that there exists an optimal range of bandgap energies to generate the highest electrical power densities. The Si bandgap (1.1 eV) is exactly amidst this range, maximizing the $P_{max,SQ}$ curve.

Modern commercial LEDs are made of a double heterojunction structure to maximize the light emission efficiency (see Fig. 2).^{12,18,19} This structure consists of a semiconductor layer sandwiched between p-type and n-type semiconductor layers with wider bandgaps, hence forming two pn junctions.

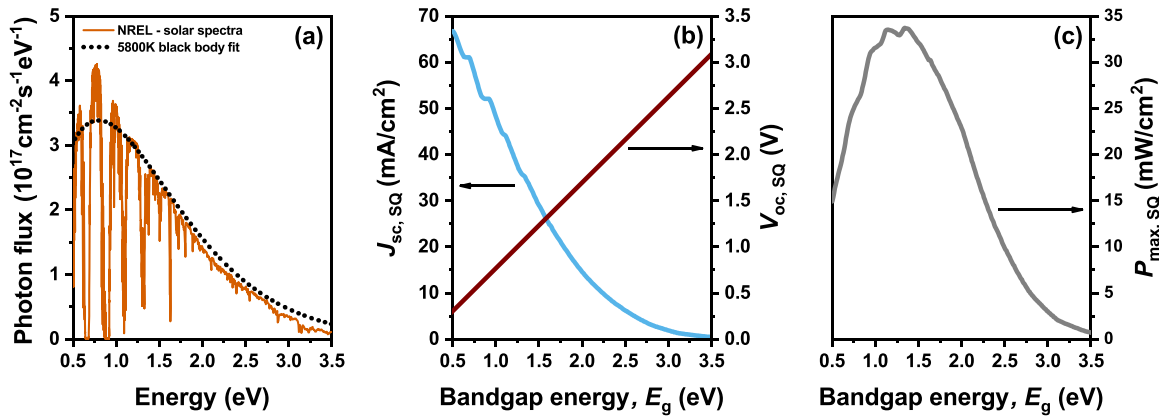


Fig. 1. (Color online) SQ theory. (a) Photon flux of the AM1.5 solar spectrum used in the model's calculations and its comparison with the spectrum of a black body at 5800 K. Both spectra are normalized such that the power density is 1000.4 W/m^2 . (b) Short-circuit current density $J_{sc,sq}$, open-circuit voltage $V_{oc,sq}$, and (c) maximum electric power density $P_{max,sq}$ as a function of the absorber bandgap energy E_g . The optimal bandgap energies for single absorber SCs are in the range of $1.1 \text{ eV} < E_g < 1.4 \text{ eV}$. Adapted from Ref. 15.

This sandwiched layer is designated as the *active layer*, and it is crucial for achieving efficient light emission, serving as the primary region where radiative recombination occurs due to carrier confinement. When forward bias is applied to the structure, the electrons (holes) in the *n*-type region (*p*-type region) will drift toward the *pn* junction and enter the active layer. Due to the lower bandgap energy of the active layer compared to the neighboring *p*- and *n*-type semiconductors, the injected charge carriers become energetically confined in this region. This bandgap difference creates an energy barrier at both junctions, preventing charge carriers from returning into the wider-bandgap materials. As a result, this carrier trapping increases the electron–hole recombination within the active layer, resulting in increased probability of radiative recombination, i.e., the emission of photons with energy approximately equal to the bandgap energy E_g of the active layer.^{12,18} The photon emission, known as electroluminescence (EL), is the fundamental mechanism behind the typical operation of LEDs.^{15,16,18} Additionally, EL can be used as a characterization technique for both LEDs and SCs by measuring emission spectra while injecting charge carriers under

forward bias, allowing one to investigate the radiative recombination mechanisms of charge carriers in the semiconductor material.¹⁵ For example, applying forward bias to a Si SC induces light emission in the near-infrared region (around 1.1 eV). In our experimental study, students will use EL spectroscopy measurements to estimate the bandgap energy E_g of the active layer for various LEDs. Given that spectroscopy is a vital part of any physics, engineering, or chemistry degree program, engaging in these measurements is highly beneficial.

The active layer of commercial LEDs is, generally, fabricated using III-V compound semiconductors.^{12,18} For red, orange, and yellow LEDs, the active layer is typically constituted from the direct bandgap semiconductor AlGaInP. By adjusting the Al/Ga ratio, the bandgap energy of the active region can be tuned, thereby modifying the emitted light wavelength. When the Al/Ga ratio exceeds 1.13, the alloy transitions to an indirect bandgap semiconductor, causing a significant drop in light emission efficiency. As a result, it becomes impractical to fabricate AlGaInP-based LEDs with emission wavelengths shorter than 570 nm. In these devices,

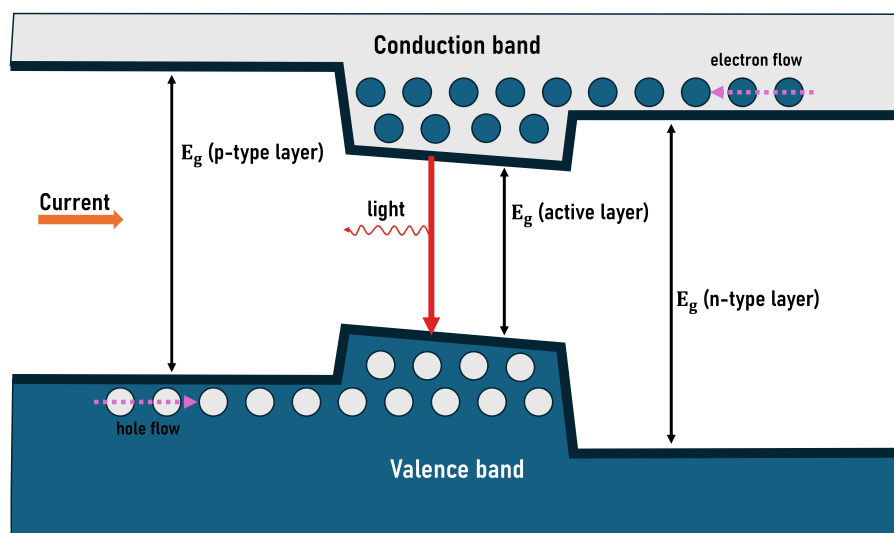


Fig. 2. (Color online) Illustration of the charge carrier concentration and current flow within an LED double heterojunction structure under forward bias. On the left side is the wide *p*-type semiconductor layer; in the center is the lower-bandgap active semiconductor layer (responsible for the light emission), and on the right is the wide *n*-type semiconductor. The full and empty circles illustrate the electrons and holes, respectively. Adapted from Ref. 18.

the surrounding n - and p -type semiconductor layers are usually made from the same AlGaInP alloy but slightly doped with other elements to be n - or p -type doped. On the other hand, for blue and green LEDs, the active layer is typically made from InGaN, where bandgap tuning is achieved by varying the In/Ga ratio. However, increasing the In content in order to shift the emission toward longer wavelengths introduces greater lattice mismatch between the active layer and the neighboring wide-bandgap GaN-based n - and p -type layers, where the doping of these GaN-based layers is achieved by adjusting the Ga/N ratio. This lattice mismatch induces strain and dangling bonds, which then leads to defects affecting LED efficiency and reliability.

Regarding the earlier discussion, double heterostructure LEDs can be considered as single-layer light absorbers, since only the active layer material has a sufficiently low bandgap energy to allow absorption of visible light and near-UV photons. Therefore, when light falls on the active layer of an LED, mobile charge carriers will be generated and, consequently, the LED will exhibit photovoltaic behavior. However, several factors limit the effectiveness of LEDs as SCs. First, the bandgap energy of the active layer is too high (~ 1.8 eV for red and ~ 2.8 eV for blue), restricting absorption to a small portion of the solar spectrum and reducing power generation accordingly with the SQ-theory predictions [see Fig. 1(c)]. Second, the active layer has a very small area, limiting the light absorption compared to commercial SCs, which are designed with large-area absorbers. Third, the electrical contacts might not be optimized to achieve optimal charge carrier extraction. Finally, the p -type and n -type regions can introduce parasitic absorption in the blue to UV range, reducing the number of photons reaching the active layer.

These differences illustrate how semiconductor junctions can be optimized for either light emission (LEDs) or light absorption (SCs). While SCs maximize absorption and carrier collection through material selection, surface passivation, and antireflective coating,¹⁵ LEDs are designed to confine carriers and enhance radiative recombination efficiency.¹⁸ However, the purpose of this work is to clarify the concept of using commercial LEDs as SCs for teaching purpose, rather than aiming for the generation of high electrical power levels. For this purpose, students will engage in measuring the current–voltage (I – V) characteristics of the commercial LEDs in the photovoltaic mode under outdoor sunlight illumination. These measurements allow students to estimate several electrical parameters and, most importantly, verify the photovoltaic behavior of common LEDs.

III. MATERIALS AND EXPERIMENTAL METHODS

For this hands-on instructional laboratory experiment, all the necessary components are inexpensive and consist of items commonly found in university teaching laboratories and electronics stores. Students will need LEDs of various colors with water-clear lens/encapsulation. Suitable options include red, orange, amber, yellow, green, cyan, light-blue, deep-blue, and violet LEDs. In this work, 5-mm LEDs of various colors were sourced from Optosupply. The specific part numbers for each LED are as follows: red (OSR5PA5111A), amber (OSY5PA5111A), green (OSG5DA5111A), and blue (OSB5SA5111A). More information about the LEDs can be found in the [supplementary material](#).

To measure the LEDs' EL spectra, a simple spectrometer (Ocean Optics USB2000+) was used, as well as a typical programmable DC power supply to apply voltage across the LED heterojunction and, thus, achieve charge carrier injection.¹⁵ To find the optimal voltage range to apply, students must refer to the LEDs' manufacturer-supplied datasheets. The experimental setup is illustrated in Fig. 3(a).

In the second part of the experiment, students measure the I – V curves of the LEDs operating in the photovoltaic mode. For these measurements, the LEDs' active layer needs to be exposed to direct sunlight. Although illumination with a typical tungsten lamp is possible, experimental results (as achieved by the authors of this work) show that only the red and amber LEDs will exhibit a measurable level of photovoltaic behavior [see Fig. S5(a) and Table S2 in the [supplementary material](#)]. This effect occurs because a tungsten lamp operating at approximately 3300 K emits a negligible photon flux in the blue to near-UV spectral region, whereas sunlight, which can be viewed as a lamp operating at 5800 K, provides a higher flux of the high-energy (green and blue) photons necessary to excite the active layer of higher bandgap LEDs. To achieve the best results, a proper laboratory solar simulator can be used. However, as most instructional laboratories do not have access to this expensive piece of equipment, we recommend that students conduct the measurements outdoors on a clear-sky day. Figure 3(b) provides a schematic of the experimental setup used to measure the I – V curves of the LEDs under illumination. For this setup, two multimeters (we used AMPROBE AM-500-EUR units), one working as a voltmeter and the other as an ammeter, a variety of resistors and potentiometers, and electrical cables are required. Students will finely adjust the circuit's resistance from 0 to infinity, while measuring the voltage and current values produced by the LED.^{5,20–22}

IV. RESULTS AND DISCUSSION

A. Optical measurements: Estimating the LED's active layer bandgap energy

Figure 4 shows the superposition of the EL spectra measured for various LEDs at room temperature. As expected, each LED spectrum shows a peak at a distinct wavelength,

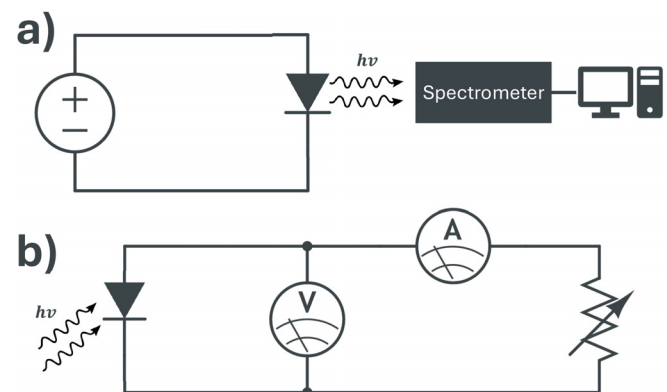


Fig. 3. Experimental setup. (a) To measure the EL spectra, students need a simple spectrometer (connected to a computer) and a programmable DC power supply. (b) To measure the I – V characteristics, students build the circuit shown using two multimeters (one working as a voltmeter and the other as an ammeter) and a variable resistor. The light emitted/absorbed by the LED is represented by the wavy arrows.

which relates to the spectral perception of color by the human eye. To estimate the bandgap energy, the wavelength peak can be converted into energy using the widely known equation $E = hc/\lambda_{\text{peak}}$, where h is Planck's constant, and c is the speed of light in vacuum. Table I exhibits, for each LED, the human-eye perceived color, the measured peak wavelength, and the active layer bandgap energy estimated from the EL spectroscopy analysis.

This experiment helps students understand the relation between bandgap energy and the LED color. Additionally, students will observe that the LED's EL spectra exhibit a broad-band profile. It must be noted that the green LED showed the largest broadening in energy units. This broadening likely relates to band-edge emission from optically active defects in the bandgap and natural broadening effects happening at room temperature.¹⁸ However, the spectra remain relatively narrow compared to the entire visible spectrum, allowing LEDs to be perceived as monochromatic by the human eye.

To further connect bandgap energy measurements to material composition, students can use relations known in the literature.^{12,18} Following the equations given in the [supplementary material](#), and using the bandgap energy estimated through the EL measurements, the ratio of Al/Ga or In/Ga of the LEDs can be estimated.

B. Electrical measurements: LED's photovoltaic behavior under sunlight incidence

The second, and most important, part of this study involves measuring and analyzing the LEDs' I-V curves under sunlight. To avoid fluctuations in the results, due to the unpredictable nature of sunlight, all measurements should be conducted within the shortest possible time span.

Figure 5 shows the I-V (bottom) and subsequently calculated P-V curves (top) for (a) red and amber and (b) green and blue LEDs under outdoor sunlight illumination. The representation was made in pairs to facilitate the graphical representation of the data points, since the measured electric currents for the green and blue LEDs are at least one order of magnitude lower than those of the red and amber ones. Also,

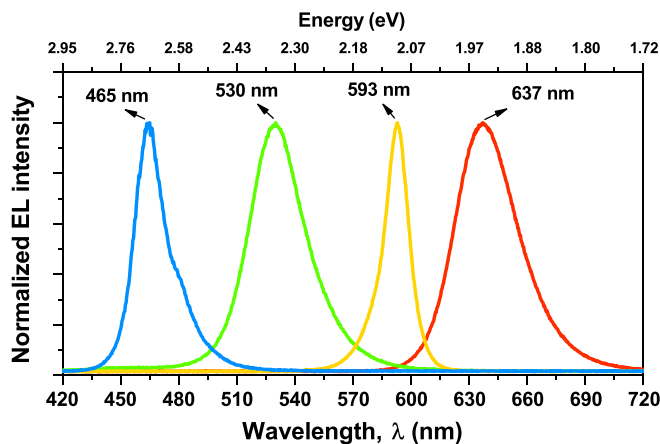


Fig. 4. (Color online) EL spectra superposition for the various LEDs considered in this work. The spectra were measured at room temperature under forward bias. The applied voltage was adjusted to ensure that all LEDs emitted a similar EL intensity when measured from the same position relative to the spectrometer's optical fiber. The measured peak wavelength values are displayed in the figure.

Table I. Color as perceived by the human eye, EL spectra peak wavelength λ_{peak} and estimated active layer bandgap energy E_g for various commercial LEDs. The measured peak wavelength values have an error of approximately 0.4 nm, which will be disregarded for simplicity.

Color	λ_{peak} (nm)	E_g (eV)
Red	637	1.95
Amber	593	2.09
Green	530	2.34
Blue	465	2.67

it must be noted that the measured current values for the green and blue LEDs are very close to the ammeter scale's lower limit ($0.1 \mu\text{A}$), resulting in a limited number of obtained data points. To verify that the LEDs were not defective and to ensure reliable results, multiple LEDs of each color were tested during the session (results not shown). Consistent current and voltage measurement between the LEDs confirmed that the LEDs used in the following experiments were not defective. This fact was also confirmed by testing the light emission.

In Fig. 5, the measured current is plotted with negative values. When a solar cell is illuminated, the photocurrent (flowing out of the cell) is conventionally considered negative, as the forward-bias current is defined as positive. Notwithstanding, both negative²³⁻²⁷ and positive^{28,29} presentation forms are common in the literature. Unlike current, where the sign depends in which direction it flows, the electrical power generated by a solar cell is always positive. Thus, power was plotted with positive values.

The results of Figs. 5(a) and 5(b) clearly demonstrate that a simple commercial LED exhibits photovoltaic behavior, functioning as a SC and challenging the misconception that LEDs are solely capable of emitting light. From the measured curves, students are able to estimate the following electrical parameters: open-circuit voltage V_{oc} , short-circuit current I_{sc} , and maximum generated power P_{max} . The estimated values for the obtained results in this work are shown in Table II.

Theoretically, the red LED should absorb a larger number of photons due to the lower bandgap energy, thus producing a higher current. However, the lower bandgap energy limits the voltage produced by the mobile charge carriers accumulation. Experimentally, the red LED exhibited higher I_{sc} and lower V_{oc} values than the amber one, which agrees with the expectations from the SQ theory, assuming that the active layer of both LEDs have an equal area (see Fig. S3 in the [supplementary material](#)). Also, the P-V curves show that the red LED produces a higher maximum electrical power P_{max} than the amber LED, which is also expected from the SQ theory, since the red LED bandgap energy is closer to the optimal bandgap energies (1.1–1.4 eV) than the amber one.

Similarly, the electrical analysis was conducted for the green and blue LEDs. The obtained V_{oc} values for the green and blue LEDs follow the bandgap energy tendency, aligning with the SQ-theory predictions. However, despite the expected decrease, the obtained values of I_{sc} and P_{max} are at least one order of magnitude lower than those obtained for the red and amber LEDs. Moreover, contrary to the SQ-theory predictions, the obtained P_{max} value for the green LED is significantly lower than the value obtained for the

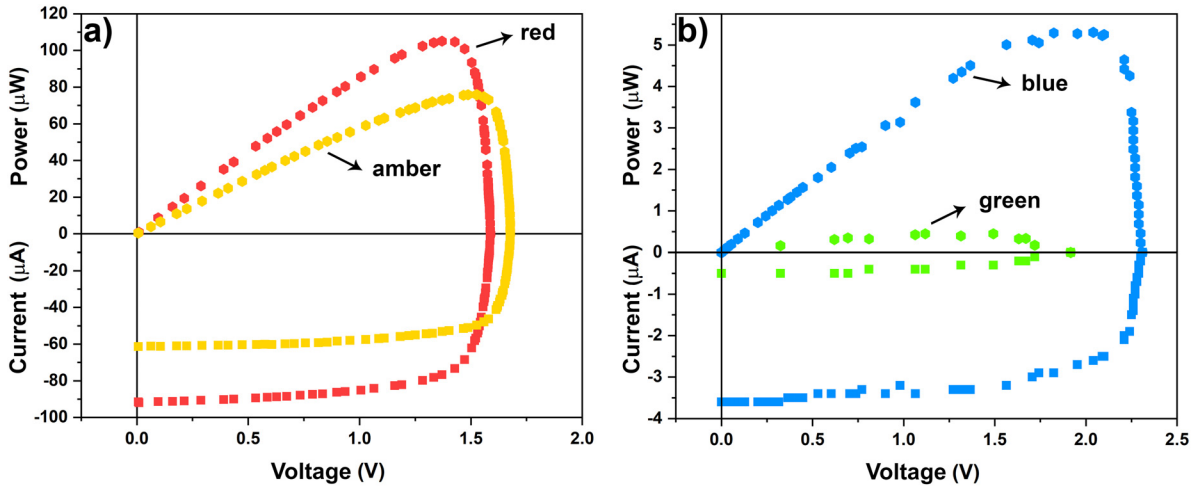


Fig. 5. (Color online) Measured I–V (bottom) and subsequently calculated P–V curves (top), for (a) red and amber and (b) green and blue LEDs under outdoor sunlight illumination. The measured current is plotted with negative values, indicating that the photocurrent flows in the opposite direction to forward-bias current.

blue one. Thus, it can be concluded that the green LED exhibits the weakest photovoltaic behavior.

The I_{sc} values for the amber, green, and blue LEDs can be compared to the I_{sc} value of the red LED by normalization. The experimentally measured I_{sc} values for the amber, green, and blue LEDs are 67%, 0.5%, and 4%, respectively, of the I_{sc} value for the red LED. However, according to the SQ-theory predictions, these values should have been approximately 80%, 50%, and 30% of the $I_{sc,SQ}$ value of the red LED. Based on this significant discrepancy observed for the green and blue LEDs, students can quickly conclude that the material system responsible for the active layer of the red and amber LEDs (typically AlGaInP) is, for photovoltaic purpose, more efficient than the material system of the green and blue LEDs (typically InGaN). The same analysis can be performed for the P_{max} values.

To convincingly demonstrate that the LEDs are generating electrical energy (thus behaving as SCs), students can connect a small electrical device to the LED terminals, while pointing it directly into the sunlight. Remarkably, instead of using a typical battery, we powered a small and simple calculator (and performed calculations) using only a single red LED as the power source. Additionally, students can assemble mini-modules comprised of several LEDs in parallel to achieve electrical current superposition and extract a higher electrical output (see Figs. S4 and S5 in the [supplementary material](#)).

C. Quantum efficiency and the LED’s green gap problem

Quantum efficiency, QE, is a term that describes the relation between mobile charge carriers and photons in an optoelectronic device. In the context of LEDs, the ratio between

Table II. Color as perceived by the human eye, active layer bandgap energy E_g , open-circuit voltage V_{oc} , short-circuit current I_{sc} , and maximum power P_{max} for the various commercial LEDs used in this work, characterized under sunlight incidence.

Color	E_g (eV)	V_{oc} (V)	I_{sc} (μ A)	P_{max} (μ W)
Red	1.95	1.59	−92.0	105
Amber	2.09	1.68	−61.3	75.8
Green	2.34	1.92	−0.5	0.4
Blue	2.67	2.31	−3.6	5.3

the number of injected mobile charge carriers to the number of photons emitted can be defined as “emission” QE. While, for SCs, the ratio between the number of incident photons to the number of mobile charge carriers generated in the absorber material and collected in the SC’s terminals can be designated as “photovoltaic” QE. Not all the alloys used for the absorber layer of a SC are equally efficient at generating mobile charge carriers upon light incidence. More detailed information could be found in Refs. 15 and 18.

The well-known “green-gap” in LED technology refers to the difficulty in developing efficient LEDs that emit light in the green region of the visible spectrum. According to the literature, the AlGaInP and InGaN material systems are capable of producing highly efficient LEDs in the red and deep-blue spectral regions, respectively. However, when both material systems are tuned to produce green LEDs, the light emission efficiency decreases significantly, leading to a drastically lower “emission” QE for these colored LEDs. As discussed in Sec. II, when tuning the AlGaInP to produce green light, the alloy transitions to an indirect bandgap semiconductor and the “emission” QE drops significantly. Similarly, in the InGaN material system, when increasing the In content in order to shift the emission toward longer wavelengths, a greater lattice mismatch results between the active layer and the neighboring n - and p -type layers.

In Sec. IV B, we found that the green LED is the least efficient in generating electrical current when functioning as a SC. The experimental measurements show that the red LED generated 263 times more power than the green LED when operating as a SC. This radical difference cannot be explained by the SQ theory. According to the SQ model, a SC absorber with a bandgap of 1.95 eV (red) should produce only about twice the electrical power produced by an absorber with a bandgap of 2.34 eV (green). The significant deviation from the model’s prediction highlights the presence of additional loss mechanisms in the green LED. Therefore, the “photovoltaic” QE must be substantially lower for the green LED. Looking at this issue the other way around, if the “photovoltaic” QE were 100%, the electrical power generated by the LEDs would follow the trend predicted by the SQ theory, and that is not the case.

Figure 6 displays the ratio between the experimentally measured short-circuit current I_{sc} and the theoretical

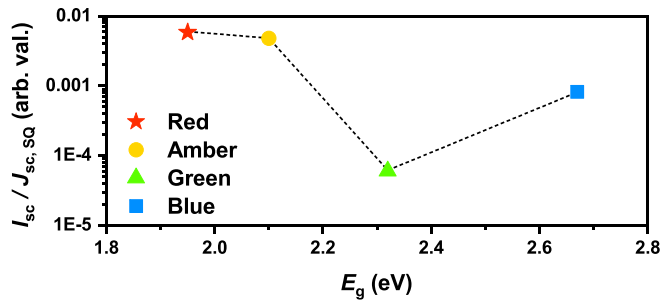


Fig. 6. (Color online) Ratio between the experimentally measured short-circuit current I_{sc} and the theoretical short-circuit current density $J_{sc,SQ}$, predicted by SQ theory for all four LEDs. This ratio is plotted against the bandgap energy of the LED's active layer. The values obtained are arbitrary since the areas of the LEDs pn junctions are unknown.

short-circuit current density $J_{sc,SQ}$, predicted by the SQ theory for all the four LEDs. This ratio is plotted against the bandgap energy of the LED's active layer. The values obtained are arbitrary since the absolute values of the LEDs' active layer areas are unknown (however, as seen in Fig. S3 in the [supplementary material](#), their sizes are relatively similar). Thus, the results for the LEDs can only be analyzed relative to one another, while an absolute comparison would require knowledge of the area of each LED.

The SQ theory assumes a “photovoltaic” QE of 100%, meaning that any photon with energy equal or greater than the bandgap energy of the absorber material will generate an electron–hole pair. The ratio $I_{sc}/J_{sc,SQ}$ approximates “photovoltaic” QE by comparing measured current to theoretical predictions. This value reflects how efficient the LED active layer is in converting the incident photons to free charge carriers collected at the device terminals. By comparing this ratio between the different LEDs, students can obtain a rough estimate of the “photovoltaic” QE of the LED acting as a SC. Since the LED areas are unknown, the results can only be compared relative to one another. In this sense, Fig. 6 shows that the red and amber LEDs have very similar “photovoltaic” QE, although slightly lower for the amber one. As expected, due to the results obtained in Sec. IV B, the “photovoltaic” QE of the blue and green LEDs are one and two orders of magnitude lower than that of the red LED, respectively.

This analysis helps students connect the lower “photovoltaic” QE of the green LED with its low “emission” QE, a key characteristic of the green-gap problem, which is well known in the literature.^{30,31} The green gap refers to the reduced emission efficiency of green LEDs due to intrinsic material limitations, such as high defect density and poor charge carrier dynamics, which hinders device performance. This aligns with the earlier discussion on lattice mismatch in the InGaN material system, where increasing the In content in order to shift emission toward the green spectrum creates strain and defects.¹⁸ These entities pose a pivotal effect in the light-to-matter interactions.

By comparing the results obtained in Fig. 6 with the literature on “emission” QE as a function of bandgap energy,^{30,31} students will recognize that the trend that they observed for the LEDs' photovoltaic performance in this experiment directly correlates with their LEDs' emission efficiency in normal operation. This observation supports the idea that the same material properties affecting LED light emission also influence photovoltaic behavior. The broader EL spectra (in energy units) for the green LED also suggests a higher

density of optical and electrically active defects in the active layer of the green LED. As stated before, this broadening is due to localized states within the bandgap that were introduced resulting from a higher density of defects in the semiconductor. Green LEDs, based on InGaN, are more prone to a higher density of defects due to the lattice mismatch between the active layer and the neighboring n - and p -type semiconductors. Additionally, students will be able to discuss that, while SQ theory is a useful theoretical model, it does not accurately reflect real-world conditions. It will become evident that factors beyond the bandgap energy of the light-absorbing material must be considered to create an accurate model for predicting the SC's efficiency.

V. CONCLUSION

This laboratory experiment demonstrates the fundamental similarities between light-emitting diodes (LEDs) and solar cells (SCs), emphasizing their common ability to generate electrical energy as a result of light absorption. Our contribution to this topic aims to clarify these concepts and enhance the understanding of various physics- and chemistry-related topics for undergraduate and graduate students.

Our experiment is accessible and cost-effective, making use of readily available components to facilitate hands-on learning for students. By using optical and electrical characterization techniques to study LEDs of various colors, students will gain insight in the relation between bandgap energy, photon wavelength, and LED color, reinforcing theoretical concepts with practical observations. While proper SCs would have been ideal for this experiment, it is challenging and costly to find SCs with a variety of bandgap energy values. The market is dominated by Si-based modules ($E_g = 1.1$ eV), with few affordable alternatives. In contrast, LEDs cover a wide range of bandgap energies and are significantly cheaper, making them a more practical choice for this experiment.

The study's findings reveal that LEDs, when exposed to sunlight, exhibit photovoltaic behavior, with notable differences in performance based on color. The studied red LED displayed higher short-circuit current I_{sc} , lower open-circuit voltage V_{oc} , and maximum electrical power outputs P_{max} than the amber, green, and blue LEDs. Considering that all LEDs have an active layer with similar area, these results align with Shockley–Queisser (SQ) theory predictions. However, significant discrepancies, such as the lower-than-expected photovoltaic performance of the green LED, reveal the complexities of real-world applications and underscore the importance of considering factors beyond bandgap energy when evaluating photovoltaic performance. The SQ theory provides an upper bond for generated electrical power density under idealized assumptions, such as perfect material quality, 100% “photovoltaic” quantum efficiency QE, and the absence of non-radiative recombination. Real-world conditions deviate due to factors like defects, surface recombination, imperfect light trapping, and parasitic absorption in non-active layers. These phenomena reduce the photovoltaic performance, highlighting the nuanced limitations of the SQ theory. Additionally, the poor photovoltaic performance of the green LED aligns with the well-known green-gap problem, which describes the difficulty in producing these LEDs with high emission efficiency.

The figures and data collected during the experiment provide a valuable educational tool, allowing students to visualize and analyze the photovoltaic behavior of different LEDs. The

results encourage critical thinking about the theoretical models and their practical implications, fostering a deeper understanding of semiconductor devices' operational principles. Overall, this work not only bridges the gap between theory and practice but also enhances the pedagogical approach to teaching semiconductor-related topics and photovoltaic physics.

SUPPLEMENTARY MATERIAL

Please click on [this link](#) to access the supplementary material for additional experimental information relating to the visual and photographic inspection of the LEDs' active layer, photographs of the LEDs' light emission, electrical characterization (I–V measurements) under tungsten lamp light, and construction and electrical characterization of modules consisting of several LEDs (PDF). The [supplementary material](#) also includes the following documents: Student Manual and Instructor Manual. These resources are designed to facilitate the integration of this experiment into existing courses. The Student Manual outlines the key learning objectives and includes guiding question to help students prepare their reports. Print readers can see the supplementary material at <https://doi.org/10.60893/figshare.ajp.c.7731920>.

ACKNOWLEDGMENTS

The authors would like to thank the Departamento de Física, Universidade de Aveiro, Portugal, for providing the necessary experimental conditions to carry out this work. T. V. Fernandes acknowledges the financial support from the Project “Agenda ILLIANCE” (C644919832-00000035—Project n° 46), financed by PRR—Plano de Recuperação e Resiliência—under the Next Generation EU initiative from the European Union, as well as the current financial support from Uppsala University.

AUTHOR DECLARATIONS

Conflict of Interest

The authors have no conflicts to disclose.

^aElectronic mail: tiagofernandes00@ua.pt and tiago.fernandes@kemi.uu.se, ORCID: 0000-0002-0192-3056.

^bORCID: 0000-0002-0419-731X.

^cORCID: 0009-0006-1613-6414.

¹International Renewable Energy Agency, *IRENA Renewable Capacity Statistics 2024* (International Renewable Energy Agency, Abu Dhabi, 2024).

²R. H. Chow, “Photovoltaic experiment using light from a solar simulator lamp,” *Am. J. Phys.* **48**(1), 48–50 (1980).

³A. Khoury, J. P. Charles, J. Charette, M. Fieux, and P. Mialhe, “Solar cells: A laboratory experiment on the temperature dependence of the open circuit voltage,” *Am. J. Phys.* **52**(5), 449–451 (1984).

⁴F. Herrmann and P. Würfel, “The semiconductor diode as a rectifier, a light source, and a solar cell: A simple explanation,” *Am. J. Phys.* **74**(7), 591–594 (2006).

⁵J. L. Maldonado, G. Ramos-Ortíz, M. L. Miranda, S. Vázquez-Córdova, M. A. Meneses-Nava, O. Barbosa-García, and M. Ortíz-Gutiérrez, “Two examples of organic opto-electronic devices: Light emitting diodes and solar cells,” *Am. J. Phys.* **76**(12), 1130–1136 (2008).

⁶R. P. Smith, A. A. Hwang, T. Beetz, and E. Helgren, “Introduction to semiconductor processing: Fabrication and characterization of p-n junction silicon solar cells,” *Am. J. Phys.* **86**(10), 740–746 (2018).

⁷G. C. Lisensky, R. L. Penn, M. J. Geselbracht, and A. B. Ellis, “Periodic properties in a family of common semiconductors: Experiments with light emitting diodes,” *J. Chem. Educ.* **69**(2), 151–156 (1992).

⁸M. G. D. Baumann, J. C. Wright, A. B. Ellis, T. Kuech, and G. C. Lisensky, “Diode lasers,” *J. Chem. Educ.* **69**(2), 89–95 (1992).

⁹E. V. Kvittingen, L. Kvittingen, B. J. Sjørnes, and R. Verley, “Simple and inexpensive UV-photometer using LEDs as both light source and detector,” *J. Chem. Educ.* **93**(10), 1814–1817 (2016).

¹⁰J. J. Wang, J. R. Rodríguez Núñez, E. J. Maxwell, and W. R. Algar, “Build your own photometer: A guided-inquiry experiment to introduce analytical instrumentation,” *J. Chem. Educ.* **93**(1), 166–171 (2016).

¹¹G. T. Cheek, “Demonstrations of frequency/energy relationships using LEDs,” *J. Chem. Educ.* **92**(6), 1049–1052 (2015).

¹²E. P. Wagner, “Investigating bandgap energies, materials, and design of light-emitting diodes,” *J. Chem. Educ.* **93**(7), 1289–1298 (2016).

¹³T. Cesin-AbouAtme, C. G. Lopez-Almeida, G. Molina-Labastida, and J. G. Ibanez, “Light-emitting diodes as voltage generators: Demonstrating the fuel cell principle with low-cost, magnetically enhanced, homemade solar electrolysis,” *J. Chem. Educ.* **98**(9), 3045–3049 (2021).

¹⁴A. Barcellos and A. L. Oliveira, “Using LEDs as solar cells is a useful tool for teaching about photovoltaic phenomena,” *Rev. Bras. Ensino Fis.* **45**, e20230216 (2023).

¹⁵Daniel Abou-Ras, Thomas Kirchartz, and Uwe Rau, *Advanced Characterization Techniques for Thin Film Solar Cells*, 1st ed. (Wiley-VCH, 2011).

¹⁶D. A. Neamen, *Semiconductor Physics and Devices*, 3rd ed. (McGraw Hill Higher Education, 2002).

¹⁷W. Shockley and H. J. Queisser, “Detailed balance limit of efficiency of p-n junction solar cells,” *J. Appl. Phys.* **32**(3), 510–519 (1961).

¹⁸E. F. Schubert, *Light Emitting Diodes*, 2nd ed. (Cambridge U. P., 2006).

¹⁹Z. I. Alferov, “Nobel Lecture: The double heterostructure concept and its applications in physics, electronics, and technology,” *Rev. Mod. Phys.* **73**(3), 767–782 (2001).

²⁰E. Duran, M. Piliouguine, M. Sidrach-de Cardona, J. Galan, and J. Andujar, “Different methods to obtain the I–V curve of PV modules: A review,” in 33rd IEEE Photovoltaic Specialists Conference, 2008.

²¹A. Malik and S. J. B. H. Damit, “Outdoor testing of single crystal silicon solar cells,” *Renewable Energy* **28**(9), 1433–1445 (2003).

²²E. Aranda, J. Gomez Galan, M. de Cardona, and J. Andujar Marquez, “Measuring the I-V curve of PV generators,” *IEEE Ind. Electron. Mag.* **3**(3), 4–14 (2009).

²³M. A. Steiner, R. M. France, J. Buencuerpo, J. F. Geisz, M. P. Nielsen, A. Pusch, W. J. Olavarria, M. Young, and N. J. Ekins-Daukes, “High efficiency inverted GaAs and GaInP/GaAs solar cells with strain-balanced GaInAs/GaAsP quantum wells,” *Adv. Energy Mater.* **11**(4), 2002874 (2021).

²⁴T. M. Schmidt, T. T. Larsen-Olsen, J. E. Carlé, D. Angmo, and F. C. Krebs, “Upscaling of perovskite solar cells: Fully ambient roll processing of flexible perovskite solar cells with printed back electrodes,” *Adv. Energy Mater.* **5**(15), 1500569 (2015).

²⁵L. Mazarella *et al.*, “Strategy to mitigate the dipole interfacial states in (i)a-Si:H/MoOx passivating contacts solar cells,” *Prog. Photovoltaics* **29**, 391–400 (2021).

²⁶M. B. Candeias *et al.*, “Cu(In,Ga)Se₂-based solar cells for space applications: proton irradiation and annealing recovery,” *J. Mater. Sci.* **58**(42), 16385–16401 (2023).

²⁷T. V. Fernandes, P. T. Patrício, A. F. Cunha, J. Gaspar, N. Catarino, M. Peres, K. Lorenz, J. P. Teixeira, P. M. P. Salomé, and J. P. Leitão, “Remarkable recovery of proton-irradiated Cu(In,Ga)Se₂-based solar cells for space applications: Thermal and light annealing treatment,” *ACS Appl. Energy Mater.* **8**(5), 2767–2778 (2025).

²⁸K. Zheng, Y. Zhou, R. Wang, G. Wang, Q. Xie, Y. Wang, L. Zheng, G. Fu, J. Pan, and S. Peng, “Rational design and optimization of the band gap and p-type doping in high-efficiency CdTe solar cells through CuSeCN treatment,” *ACS Appl. Mater. Interfaces* **17**(6), 9207–9218 (2025).

²⁹D. Jia, J. Chen, J. Qiu, H. Ma, M. Yu, J. Liu, and X. Zhang, “Tailoring solvent-mediated ligand exchange for CsPbI₃ perovskite quantum dot solar cells with efficiency exceeding 16.5%,” *Joule* **6**(7), 1632–1653 (2022).

³⁰M. Auf der Maur, A. Pecchia, G. Penazzi, W. Rodrigues, and A. Di Carlo, “Efficiency drop in green InGa_N/Ga_N light emitting diodes: The role of random alloy fluctuations,” *Phys. Rev. Lett.* **116**(2), 027401 (2016).

³¹B. Karadza *et al.*, “Bridging the green gap: Monochromatic InP-based quantum-dot-on-chip LEDs with over 50% color conversion efficiency,” *Nano Lett.* **23**(12), 5490–5496 (2023).